iScience

CellPress
OPEN ACCESS

Article

Extended SARS-CoV-2 RBD booster vaccination induces humoral and cellular immune tolerance in mice

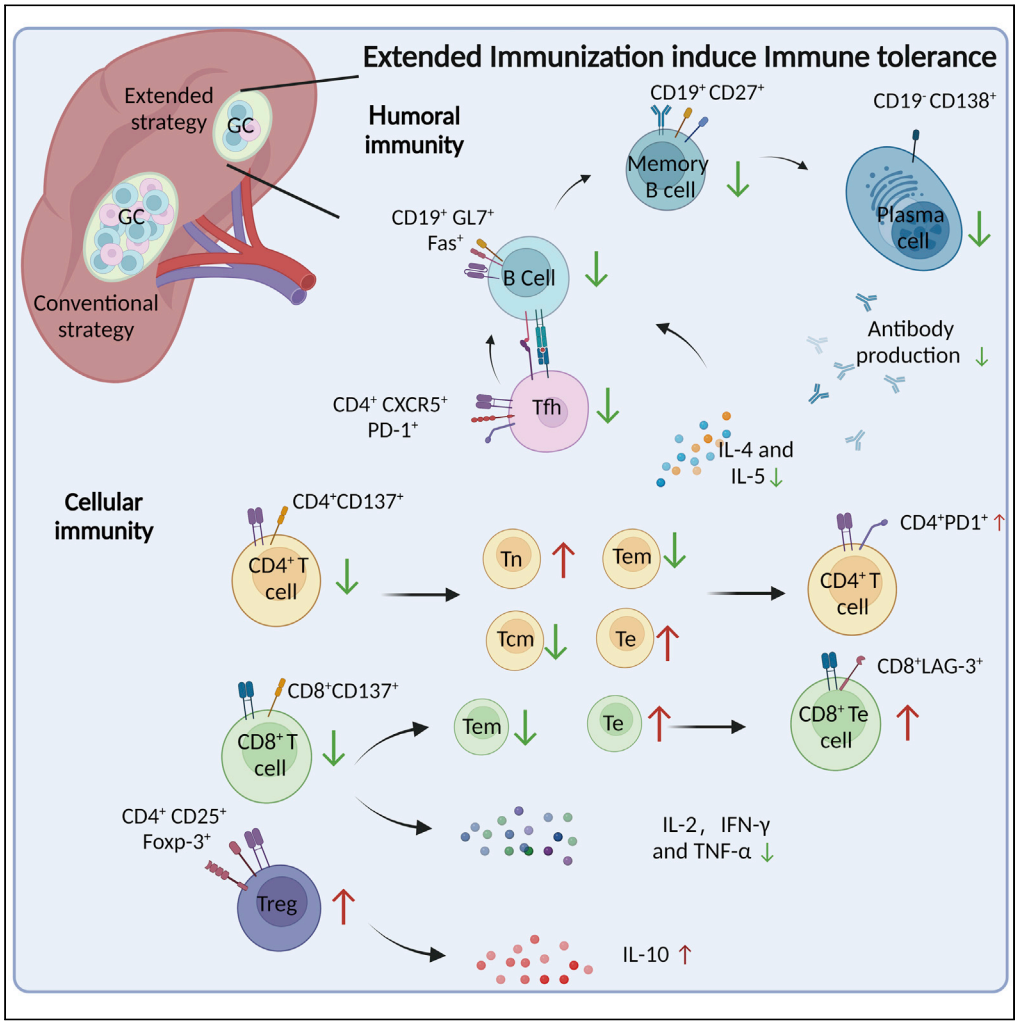

Feng-Xia Gao, Rui-Xin Wu, Mei-Ying Shen, ..., Qian Chen, Wang Wang, Ai-Shun Jin

wwang@cqmu.edu.cn (W.W.)
aishunjin@cqmu.edu.cn (A.-S.J.)

Highlights

Extended immunizations impaired the serum neutralization activity

Extended immunizations suppressed the formation of germinal center

Extended immunizations inhibited the activation of $CD8^+$T cells

Gao et al., iScience 25, 105479
December 22, 2022 © 2022
https://doi.org/10.1016/j.isci.2022.105479

iScience

CellPress
OPEN ACCESS

Article

Extended SARS-CoV-2 RBD booster vaccination induces humoral and cellular immune tolerance in mice

Feng-Xia Gao,[1,2,4] Rui-Xin Wu,[1,2,4] Mei-Ying Shen,[3] Jing-Jing Huang,[1,2] Ting-Ting Li,[1,2] Chao Hu,[1,2] Fei-Yang Luo,[1,2] Shu-Yi Song,[1,2] Song Mu,[1,2] Ya-Nan Hao,[1,2] Xiao-Jian Han,[1,2] Ying-Ming Wang,[1,2] Luo Li,[1,2] Sheng-Long Li,[1,2] Qian Chen,[1,2] Wang Wang,[1,2,*] and Ai-Shun Jin[1,2,5,*]

SUMMARY

The repetitive applications of vaccine boosters have been brought up in face of continuous emergence of SARS-CoV-2 variants with neutralization escape mutations, but their protective efficacy and potential adverse effects remain largely unknown. Here, we compared the humoral and cellular immune responses of an extended course of recombinant receptor binding domain (RBD) vaccine boosters with those from conventional immunization strategy in a Balb/c mice model. Multiple vaccine boosters after the conventional vaccination course significantly decreased RBD-specific antibody titers and serum neutralizing efficacy against the Delta and Omicron variants, and profoundly impaired $CD4^+$ and $CD8^+$T cell activation and increased PD-1 and LAG-3 expressions in these T cells. Mechanistically, we confirmed that extended vaccination with RBD boosters overturned the protective immune memories by promoting adaptive immune tolerance. Our findings demonstrate potential risks with the continuous use of SARS-CoV-2 vaccine boosters, providing immediate implications for the global COVID-19 vaccination enhancement strategies.

INTRODUCTION

Vaccines have played a center role in the protective strategy for COVID-19. Majority of COVID-19 vaccines with emergency use authorization from the World Health Organization contain a minimum of the receptor binding domain (RBD) of the SARS-CoV-2 Spike protein. Conventional courses of these vaccines have been shown with advanced benefits against SARS-CoV-2, but their neutralizing efficacy have continuously been challenged by the frequent emergence of mutational variants (Chakrabarti et al., 2022; Thiruvengadam et al., 2022; Zhou et al., 2021). Since late 2021, the SARS-CoV-2 Omicron variant has overtaken the global dominance and epidemiology studies have identified substantial levels of vaccine breakthrough infections and reinfections (Atmar et al., 2022; Walls et al., 2022). Encountering these issues, the use of booster vaccinations has been authorized for adults after completion of the basic vaccination (Tanne, 2022). Accumulating evidence showed that the use of the first vaccine booster dose was safe and effective, and it could produce high titers of neutralizing antibodies with improved efficacy against Omicron variants (Cerqueira-Silva et al., 2022; Elliott et al., 2022). However, the serum protection after one booster vaccination was shown to decline with time, which again rendered the immunized individuals prone to continuous risk from newly emerged SARS-CoV-2 variants. Thus, the administration of a second booster vaccine or, possibly, routine vaccination with boosters was brought to light, for which scarce information was available. More information was needed to properly address relevant questions in the practical field of COVID-19 prophylaxis, such as the recommended condition for the use of additional booster vaccines, the suggested number of enhancement shots to be given and the potential adverse effects of continues administration of booster vaccines.

After subcutaneous or intramuscular injection, soluble antigens of vaccines will be presented to activation B cells to form germinal centers, and further differentiate into plasma cells and memory cells secreting antigen specific antibodies (Lederer et al., 2022; Young and Brink, 2021). Meanwhile, processed T cell epitopes on vaccines are presented by MHC-I molecules to T cell surface receptors (TCRs) and activate

[1]Department of Immunology, College of Basic Medicine, Chongqing Medical University, ChongQing 400010, China

[2]Chongqing Key Laboratory of Basic and Translational Research of Tumor Immunology, Chongqing Medical University, ChongQing 400010, China

[3]Department of Endocrine Breast Surgery, the First Affiliated Hospital of Chongqing Medical University, ChongQing 400010, China

[4]These authors contributed equally

[5]Lead contact

*Correspondence: wwang@cqmu.edu.cn (W.W.), aishunjin@cqmu.edu.cn (A.-S.J.)

https://doi.org/10.1016/j.isci.2022.105479

T cells, which can differentiate into effector T cells and exert protective cellular immunity with productions of toxicity molecules (Fahrner et al., 2022; Naranbhai et al., 2022). One of the major concerns associated with continuous immunization with booster vaccines is the relative limited response window of systematic immunity to the same stimuli. It has been reported that foreign antigen stimulation can induce immune tolerance, which is manifested as inability or low efficiency to produce antigen-specific antibodies and to activate effector T cells (Lin et al., 1998; Rizzuto et al., 2022) (Han et al., 2013). Presently, it is unclear whether extended administration of RBD vaccine boosters can re-establish protective immunity or is prone to induce immune tolerance.

Here, we performed longitudinal and lateral assessment of the immune responses to an extended course of booster vaccine with RBD recombination protein in a Balb/c mouse model. We found that the conventional immunization course could stimulate sustained levels of neutralizing antibodies and promote the antigen specific $CD4^+$ and $CD8^+$T cell reactivity. However, continued vaccination promoted the formation of a prominent adaptive immune tolerance and profoundly impaired the established immune response with the conventional course, evidenced by significant reductions in antigen specific antibody and T cell response, a loss of immune memory and form of immunosuppression micro-environment. Our findings demonstrated the potential risks associated with an extended vaccine booster course of SARS-CoV-2 vaccination, with immediate implications for the strategic use of homology booster vaccines.

RESULTS

Extended immunization did not enhance RBD specific antibody production in mice

To determine whether vaccine boosters could generate beneficial effects, six-week-old female Balb/c mice were given additional doses of RBD vaccine (Extended group) following conventional strategy (Conventional group) of four times of immunization with highly purified SARS-CoV-2 RBD recombination protein (Figure 1A). As previously reported (Gao et al., 2021), we found that the levels of RBD-specific IgG antibodies were dose-dependently increased with a dosing interval of 2–3 weeks (Figure 1B). Specifically, a steady level of antibody production was observed with the fourth immunization, which was sustained over the following 6 weeks (Figure 1B). However, subsequent immunization gradually reduced the titer of RBD-specific IgG antibodies, and a significant difference could be detected after the second injection of RBD booster vaccines (Figures 1B and 1C). Because serum IgG subclass distribution is indicative of Th1- or Th2 (T helper cells, Th) biased immunity, we analyzed the IgG subclass antibody responses induced by the RBD vaccine. ELISA results showed that both RBD-specific IgG1 and IgG2a were detected in the serum from immunized mice. IgG1 titer was significantly higher than that of IgG2a, indicating that the RBD vaccine induced a Th2-like response by preferentially potentiating serum IgG1 antibody (Figures 1D and 1E). IgG1 titer in mice immunized by multiple boosters was significantly lower than that without booster. These results suggested that the RBD vaccine could stimulate the production of RBD-specific antibodies with a dominance of the Th2-type, whereas the addition of RBD booster vaccines did not enhance RBD specific antibody production in mice.

Extended immunization reduced serum neutralizing antibody responses

Next, we determined the neutralizing potential of these RBD-specific IgG antibodies from immunized mice serum. Results from the competitive ELISA showed that the serum from mice immunized with the RBD exhibited competitive efficacy over hACE2 (Figure S1A). Although the serum from both groups could reach close to 100% competitive binding to RBD at high concentrations, the extended immunization course significantly reduced the inhibitory effect at higher dilution folds comparing to the conventional vaccination group (Figure S1A). Furthermore, we assessed the neutralizing antibody activity of the RBD immunized mice serum against pseudo-viruses of SARS-CoV-2 and its newly emerged mutational variants. We observed that serum of both immunized groups exhibited neutralizing efficiency as shown from the results of the pseudo-viruses neutralization experiments (Figures 2A–2C, S1B and S1C). We found a range of 2.5- to 4-fold reduction in the geometric mean titers against Delta and Omicron comparing to the wild-type pseudo-viruses (Figures 2A–2C). To be noted, there was a significant reduction in the neutralizing capability of mice serum from the extended group against all three types of pseudo-viruses, as indicated by lower IC_{50} corresponding to each test (Figures 2A–2C). Together, the above results suggested that immunization with RBD recombination protein could yield neutralizing antibody response in Balb/c mice against SARS-CoV-2 and its variants, which might be severely impacted by extended administration of vaccine boosters.

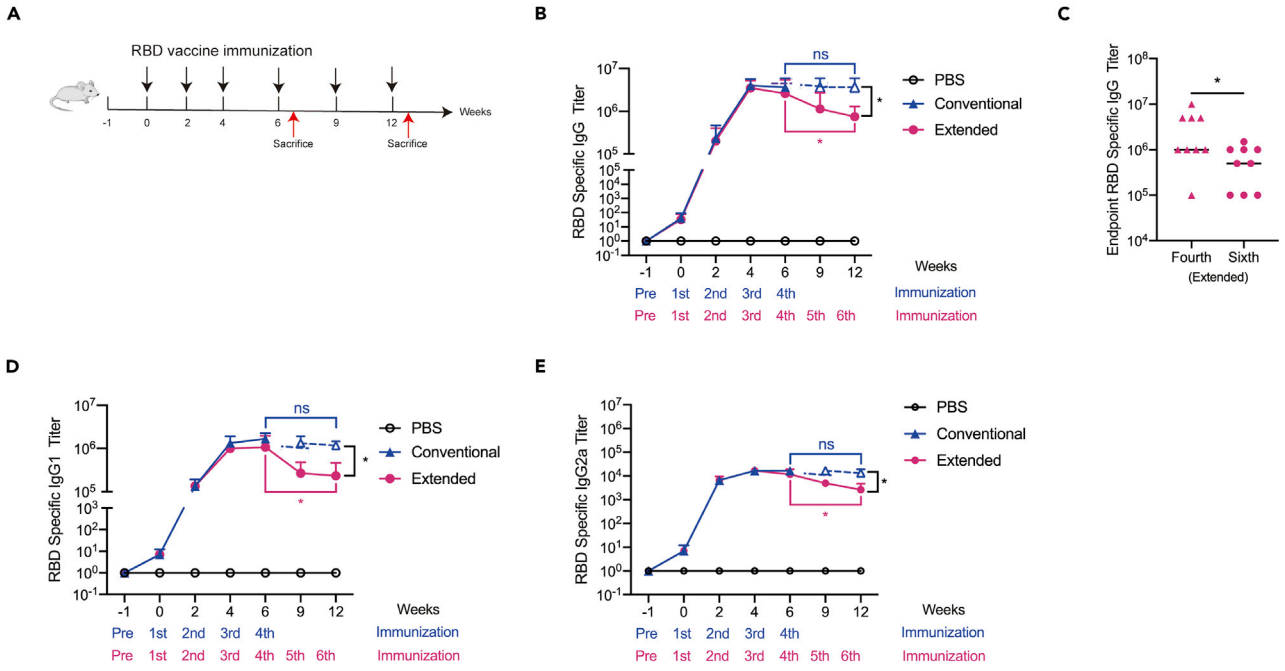

Figure 1. Extended immunization did not enhance RBD specific antibody production in mice

(A)The conventional or extended RBD vaccine immunization strategy. Black arrows represent 50 μg RBD injection. Red arrows represent mice sacrifice on the seventh day after the last immunization. Tail vein peripheral blood was collected from mice on the 10th day after each immunization. Peripheral blood was collected on the seventh day before the first immunization as the negative control.

(B) RBD-specific IgG antibody titers were tested by ELISA in mice sera taken 10 days following each injection. (N = 3).

(C) RBD binding IgG antibody titers were tested by ELISA in mice sera taken 10 days following the fourth and sixth immunization. Points represent individual mice. Data were presented as mean ± SEM.

(D) RBD-specific IgG1 antibody titers were tested by ELISA in mice sera taken 10 days following each vaccination. (N = 3).

(E) RBD-specific IgG2a antibody titers were tested by ELISA in mice sera taken 10 days following each immunization. (N = 3). *p< 0.05. ns represented non-significant. *p< 0.05, **p< 0.01, ***p< 0.001, ****p< 0.0001. ns represented non-significant.

Extended immunization inhibited the production of RBD-specific memory B cells

To explore potential mechanisms of neutralizing antibody impacted by extended administration, flow cytometric analysis was performed with total lymphocytes from the blood of immunized mice one week after the last injection of each group. The results revealed that the proportions of the CD19^{-} CD138^{+} plasma cells were significantly elevated in both groups, whereas marked reduction was observed when the immunization course was extended (Figure 3A). Also, the proportion of memory B on day 7 after the last immunization was determined by flow cytometric analysis with mice spleen samples. We found that the population of CD19^{+} CD27^{+} B cells were significantly enlarged in both two immunized group relative to the PBS control, whereas a marked reduction in the proportion of memory B cells was detected from the extended group comparing with the conventional vaccination samples (Figure 3B). Memory B cells can be induced differentiate into plasma cells via co-stimulation with a TLR receptor agonist R848 and IL-2. The antibodies secreted by memory B cell were detected by ELISPOT and ELISA assay, respectively. In accordance, the results from ELISPOT and the ELISA assay demonstrated that both conventional and extended immunizations could efficiently induce the production of RBD-specific memory B cells with the latter at a significantly lower level (Figures 3C, 3D and S1D). As B cell proliferation and differentiation are promoted by IL-4 and IL-5, we also analyzed the levels of these cytokines in the serum of immunized mice by ELISA. The results showed that RBD recombination proteins could promote significant increases in the productions of IL-4 and IL-5, whereas the serum levels of either IL-4 or IL-5 were comparatively lower with extended vaccination (Figures 3E and 3F). The above information demonstrated that additional RBD booster vaccines might result in a loss of RBD-specific humoral immunity and promote the immune tolerance.

Extended immunization suppressed the formation of the germinal center

After antigen exposure, activated antigen-specific B cells induce some previously activated T cells to differentiate into Tfh cells, which express high levels of the chemo-kine receptor CXCR5, are drawn into

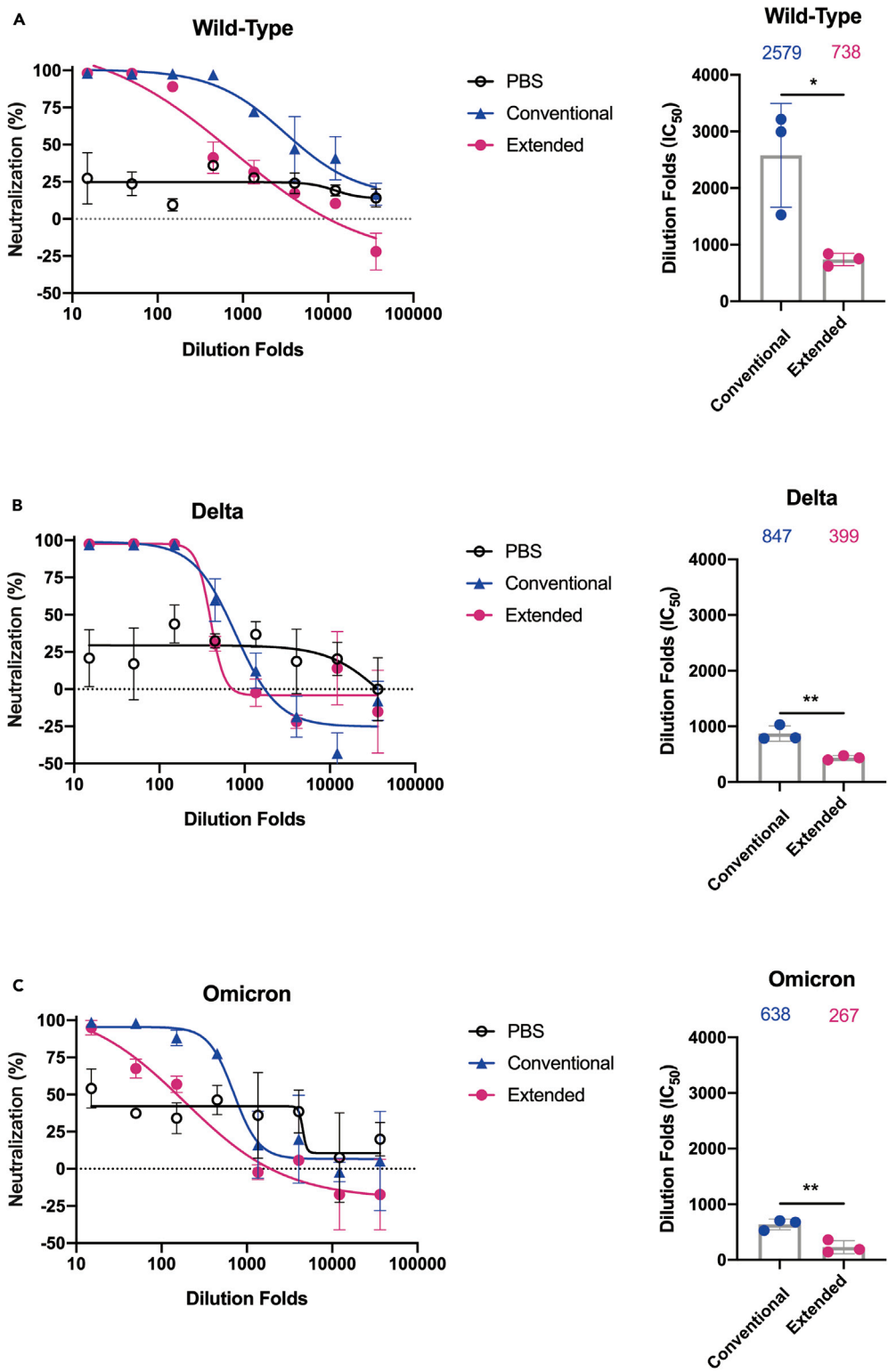

Figure 2. Extended immunization reduced serum neutralizing antibody responses

Pseudo-viruses neutralization curves for SARS-CoV-2 (wild-type) (A), Delta (B) and Omicron (C) strains by mice sera taken 10 days following the last dose of the conventional group or extended RBD vaccination. Comparison of neutralization titers between SARS-CoV-2 (wild-type) and two variant strains for the conventional and extended vaccine serum: the

Figure 2. *Continued*
Wilcoxon matched-pairs signed rank test was used for the analysis and two-tailed p values was calculated; mean values were indicated above each column. Points represent individual mice in (A), (B) and (C). Data were presented as mean ± (SEM). Representative data of two independent experiments were shown. *p< 0.05, **p< 0.01. ns represented non-significant.

lymphoid follicles, and play critical roles in germinal center formation and function. A further investigation with the formation of the germinal center was conducted to evaluate the efficiency of GC B cells differentiating into memory B cells and plasma cells that confer on the host effective long-lived humoral immunity after antigenic stimulation. Flow cytometric analysis of mice spleen samples identified a significant elevation in the proportion of $CD19^+$ $GL7^+$ Fas^+ B cells in the conventional immunized group (Figure 4A). As expected, the germinal center reaction was abolished by the extended immunization, to a level almost similar as the PBS control (Figure 4A). In parallel, the expression of the germinal center B cell marker PNA was detected by immunofluorescent staining. We found that positively stained B cells of mice spleen were remarkably reduced in the extended group, in contrast to those from animals with conventional vaccination, confirming that the formation of GC was impaired by two doses of booster vaccine. (Figure 4B). We also analyzed the proportion of $CD4^+$ $CXCR5^+$ $PD\text{-}1^+$ Tfh cells in the spleen of immunized mice and found that extended immunization decreased the population of these Tfh cells to a level like those from the PBS control, in contrast to the significant elevated Tfh populations from the conventional group (Figure 4C). Collectively, these results confirmed that inclusion of RBD booster vaccine after a normal course of immunization could not induce and elevate the germinal center responses in mouse spleen, suggesting that multiple boosters might induce tolerance rather than immune responses.

Extended immunization inhibited the activation of $CD4^+$T cell immune responses

With the observed disadvantages in the humoral immunity caused by extended immunization, we moved on to determine whether there were any differences in the cellular immune responses to the two vaccine courses. The activation of $CD4^+$T cell was analyzed by flow cytometric analysis of corresponding markers. Both immunization courses could significantly elevate the proportions of $CD69^+$ or $CD137^+$ $CD4^+$T cells, whereas the extended vaccination caused over 40% reduction in splenic $CD4^+$T cell activation (Figures 5A and 5B). A detailed study of the T cell subsets in the $CD4^+$T cells revealed that the proportion of effector memory T cells (Tem) and central memory T cells (Tcm) in $CD4^+$T cells in the extended group was sharply decreased relative to that from the normal group, along with relatively increases in naive T cells (Tn) population. Specially, we observed that the frequency of $CD4^+$ Te cells significant elevates in the extended group. (Figures 5C and S2A).

In addition, we evaluated the expressions of exhaustion markers in the $CD4^+$T cells within mouse splenocytes on day 7 after the last immunization. Flow cytometric results showed that the proportions of $PD\text{-}1^-$ $LAG\text{-}3^-$ $CD4^+$T cells were significantly decreased with extended immunization comparing to the conventional vaccination, whereas the latter group exhibited no obvious difference from the PBS control group (Figures 5D and S2B). Moreover, we found that extended immunization significantly induced the percentages of the $PD\text{-}1^+$ $CD4^+$T cells, relative to the conventional vaccination or the PBS control (Figures 5D and S2B). No apparent variations were detected for the $PD\text{-}1^-$ $LAG\text{-}3^+$ $CD4^+$T cells among all groups (Figures 5D and S2B). Besides, we confirmed that the enhanced surface expression of both PD-1 and LAG-3 was directly proportional to an increased Te proportion of $CD4^+$T cells in the extended immunization group (Figures S2C and S2D). These data suggested that additional vaccine boosters to the conventional immunized course could promote $CD4^+$T cell exhaustion. To examine the involvement of the regulatory T cell (Treg) population in the reduced cellular immunity associated with extended immunization, we determined the proportion of Treg cells in mice splenocytes a week after the last immunization. The results from flow cytometric analysis showed that a higher percentage of $CD4^+$ $CD25^+$ $foxp\text{-}3^+$ Treg cells were detected in the extended vaccination group, compared with the normal group and the PBS control group (Figure 5E). Further, we tested the serum level of IL-10, which was mainly secreted by Treg cells. The ELISA results showed that higher amount of IL-10 was detected in samples from the extended vaccination group than the other two groups, which was consistent with the increased percentile of Treg cells (Figure 5F). These data suggested Treg cells might play an important role in the immune tolerances to the extended immunization with RBD vaccines.

Extended immunization inhibited $CD8^+$ T cell-mediated immune response

To investigate the effect of vaccine boosters on $CD8^+$T cells, we studied the secreted levels of the effector cytokines one week after the last immunization. Serum concentrations of IL-2, IFN-γ and TNF-α were

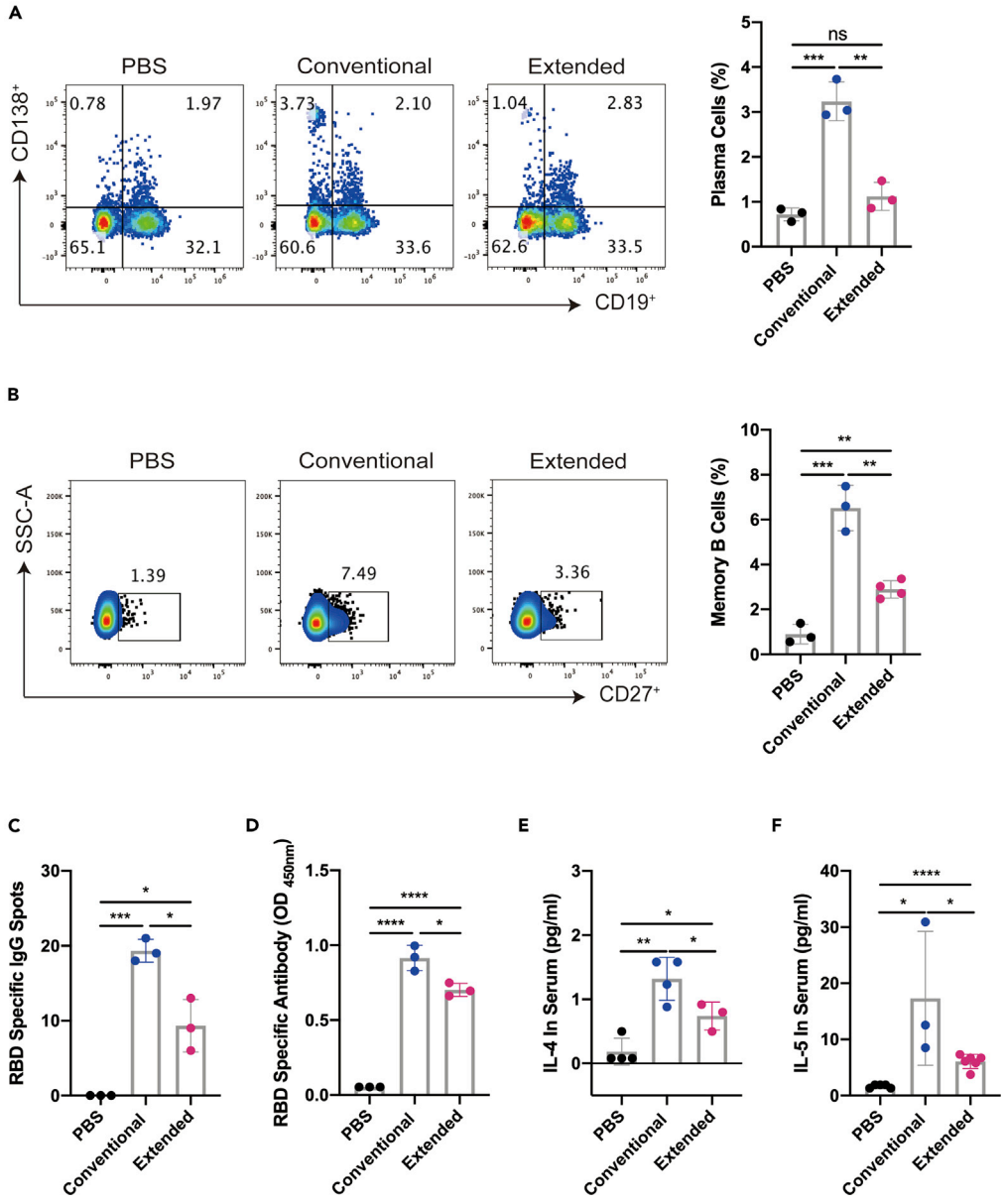

Figure 3. Extended immunization inhibited the production of RBD-specific memory B cells

(A) The ratio of $CD19^{-}$ $CD138^{+}$ plasma cells of lymphocytes were detected by flow cytometry in the blood on the seventh day after the last immunization.

(B) The percentages of $CD19^{+}$ $CD27^{+}$ memory B cells (gated on $CD19^{+}$ B cells) from the splenocytes were detected by flow cytometry on the seventh day after the last immunization.

(C) R848 (2 μg/mL) combined with 100 U/mL mouse IL-2 were stimulated to induce memory B cells to differentiation into plasma cells, on day 7 after the last immunization. ELISPOT results were showed as the numbers of RBD-specific IgG spots per 5×10^5 splenocytes of each mouse subtracted the numbers from the corresponding DMSO groups. The stimulation with an equal volume of media was performed as the negative control. Data were representative of two independent experiments.

(D) RBD-specific IgG antibodies in the supernatant of 5×10^5 splenocytes per mL were detected by ELISA. IL-4 (E) and IL-5 (F) in the serum were detected by ELISA on the seventh day after the last immunization. Data were presented as mean ± SEM Representative data of two independent experiments were shown. *p< 0.05, **p< 0.01, ***p< 0.001, ****p< 0.0001. ns represented non-significant.

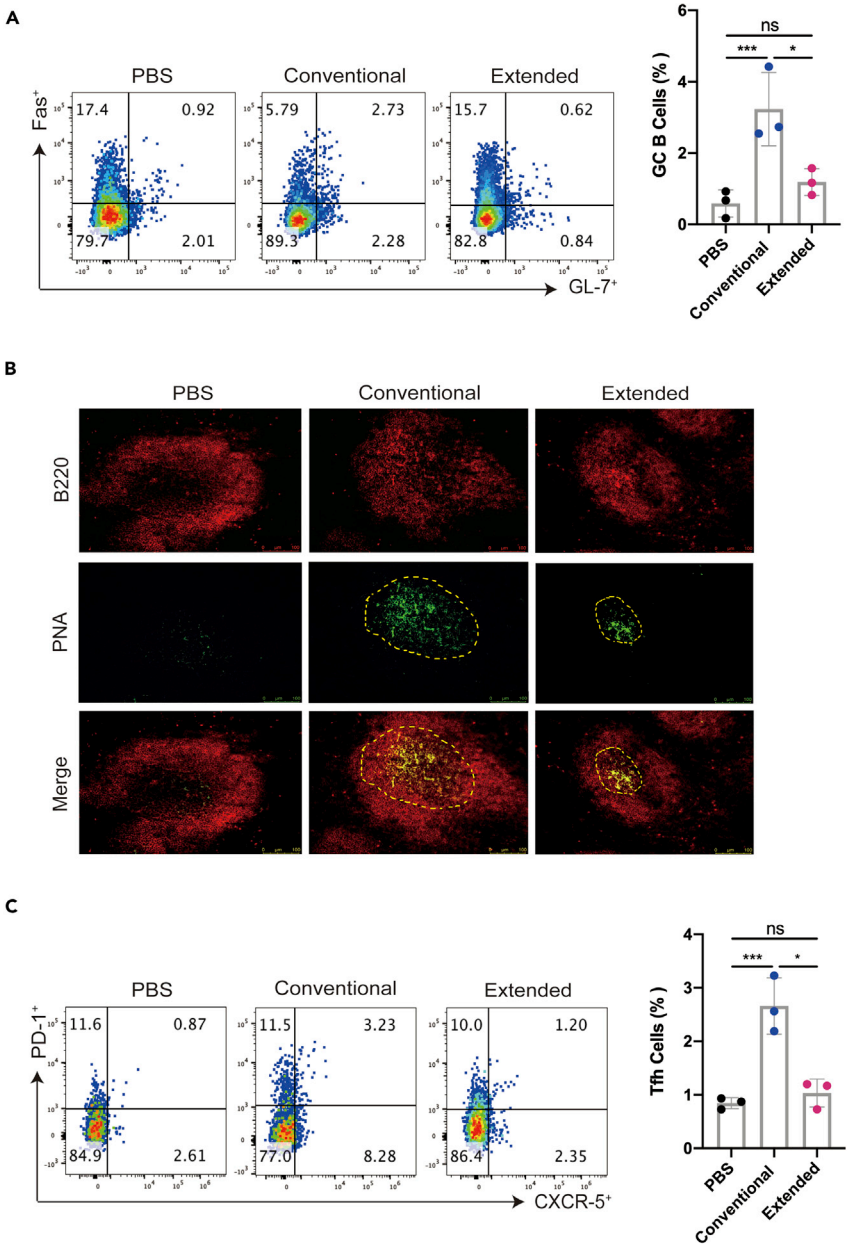

Figure 4. Extended immunization suppressed the formation of the germinal center

(A) The percentages of Fas$^+$ GL-7$^+$ B cells (gated CD19$^+$ B cells) from the splenocytes on the seventh day after the last immunization were detected by flow cytometry.

(B) On the seventh day after the last immunization, the frozen tissues of the mouse spleens were stained with PNA (green) and B220 (red). The scale bar represented 75 μm, and the pictures were analyzed by ImageJ software.

(C) The percentages of PD-1$^+$ CXCR5$^+$ Tfh cells from the splenocytes were detected by flow cytometry and shown in gated CD4$^+$T cells. Points represent individual mice in (A) and (C). Data were presented as mean ± SEM *p< 0.05, ***p< 0.001. ns represents non-significant.

significantly increased by both immunization courses, indicating a functional activation of CD8$^+$T cells (Figures 6A–6C). But the extended vaccination profoundly reduced the secretion of all three cytokines than the conventional immunization (Figures 6A–6C). To confirm these observations were the result of a SARS-CoV-2 RBD specific responses of CD8$^+$T cells, we applied a short peptide containing the sequence corresponding to a 9 amino acid region (named P45) that had been recently identified as an HLA-A*24:02 CD8$^+$T cell epitope (25), which can be crossly recognized by mouse CD8$^+$T cells. Splenocytes isolated from

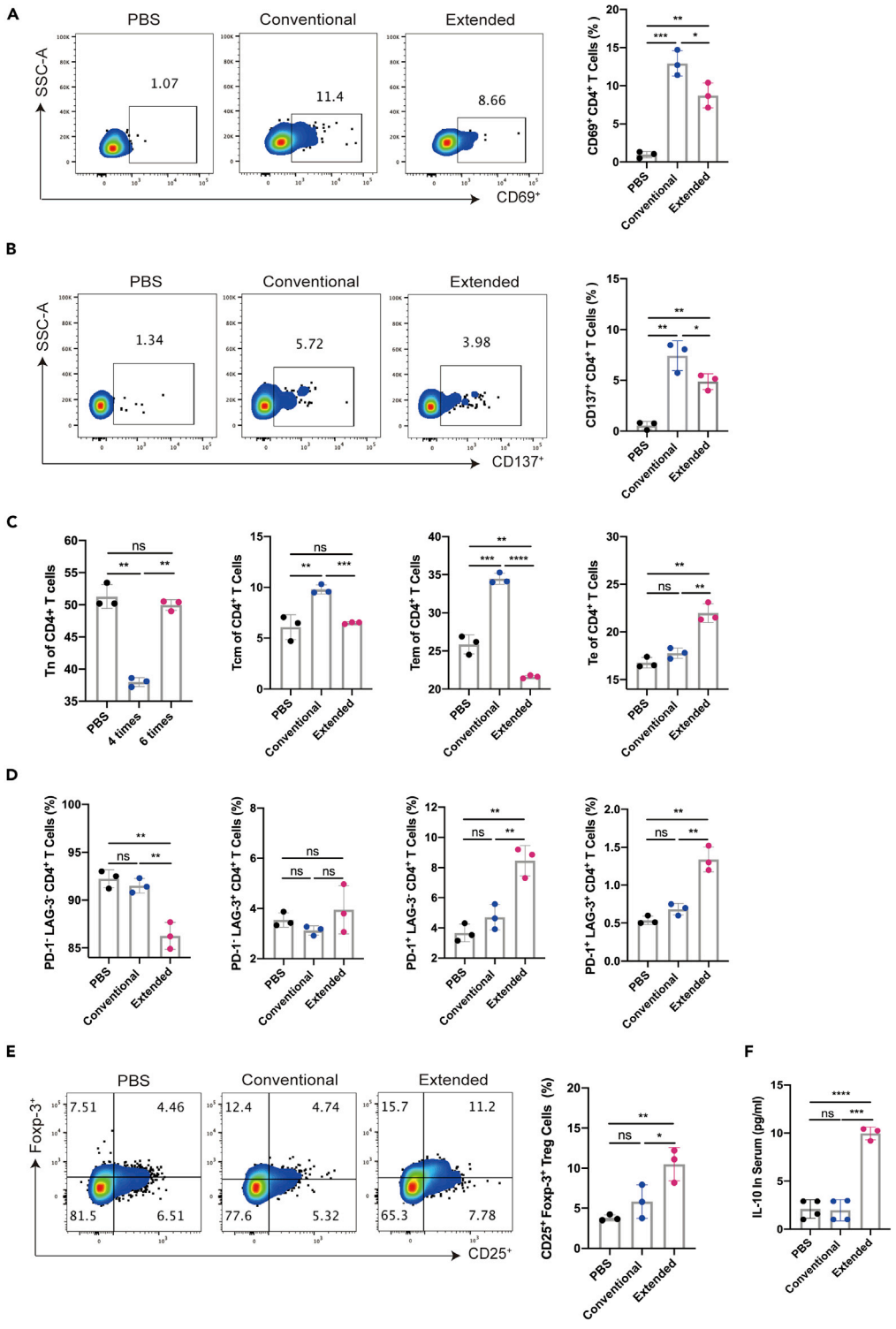

Figure 5. Extended immunization inhibited the activation of CD4$^+$T cell immune responses

The expression of CD69 (A) and CD137 (B) (gated on CD4$^+$T cells) were detected by flow cytometry on the seventh day after the last immunization.

(C) The ratio of Tn (CD62L$^+$ CD44$^-$), Te (CD62L$^-$ CD44$^-$), Tem (CD62L$^-$ CD44$^+$) and Tcm (CD62L$^+$ CD44$^+$) of CD4$^+$T cells were detected by flow cytometry on day 7 after the last immunization.

Figure 5. *Continued*
(D) The expression of PD-1 and LAG-3 (gated on $CD4^+$T cells) were detected by flow cytometry on day 7 after the last immunization.
(E) The ratio of Treg (gated on $CD4^+$) was detected by flow cytometry on the seventh day after the last immunization. IL-10 (F) in the immunized serum were detected on the seventh day after the last immunization. Data were presented as mean ± SEM *p< 0.05, **p< 0.01, ***p< 0.001, ****p< 0.0001. ns represented non-significant.

the immunized mice were stimulated by the P45 peptide for 24 h before subjected to be examined for T cell activation. Flow cytometric analysis showed that P45 enhanced the expression profile of both CD69 and CD137 in the $CD8^+$T cells, whereas splenocytes from the extended group demonstrated a remarkable lower expression level of both activating markers than those from the conventional vaccination group (Figure 6D, 6E, S3A and S3B).

Next, we studied the sub-types of $CD8^+$T cells associated with different immunization courses. Compared with the PBS group, the percentage of Tem in the extended group was significantly decreased, along with significant increase in the Te sub-population and barely any changes in the proportions of Tn and Tcm (Figures 6F and S3C). Particularly, there was more than 50% reduction in the Tem population from mice of the extended vaccination group than the conventional group, with no obvious differences in the percentile of other $CD8^+$T cell subtypes (Figure 6F).

It has been reported that repeated antigen stimulation induces the exhaustion of $CD8^+$T cells; therefore, we tested whether there were any differences in exhaustion marker levels between two immunization courses. We found that the cell surface expressions of PD-1 and LAG-3 on $CD8^+$T cells from mouse splenocytes were evidently higher in the extended vaccination group, comparing to either the conventional group or the PBS control (Figure 6G and S3D). Concomitantly, the proportion of $PD\text{-}1^-$ $LAG\text{-}3^-$ $CD8^+$T cells in the extended group was significantly less than the other groups (Figure 6G). The expressions of PD-1 and LAG-3 on the Te subsets of $CD8^+$T cells were further analyzed, and we found that the highest level of LAG-3 was expressed in the Te subsets of $CD8^+$T cells from samples with prolonged immunization (Figures S3E and S3F). These data indicated that continues administration of RBD booster vaccines could lead to reduced $CD8^+$T cell activation with increased exhaustion. Overall, our findings evidenced the potential risk of adaptive immune tolerance from prolonged course of immunization with homologous vaccine boosters, and suggested that the applications of multiple booster vaccines with protective intent should be preceded with caution.

DISCUSSION

Currently, vaccination against COVID-19 has been promoted worldwide, although sustained protection against the newly emerged SARS-CoV-2 variant strains has been continuously challenged. Clinical evidence has proven that the inclusion of an additional booster vaccine can re-stimulate the protective immune response (Cheng et al., 2022; Gruell et al., 2022). Whether such re-establishment of vaccine-induced immune response could be repeated by continued application of boosters is being questioned, yet largely unknown at present. Here, we compared the effects of repeated RBD vaccine boosters with a conventional immunization course to those with an extended vaccination strategy, in a Balb/c mice model. We found that the protective effects from the humoral immunity and cellular immunity established by the conventional immunization were both profoundly impaired during the extended vaccination course. Specifically, extended vaccination not only fully impaired the amount and the neutralizing efficacy of serum RBD-specific antibodies, but also shortened the long-term humoral memory. This is associated with immune tolerance in germinal center response, along with decreased numbers of spleen germinal center B and Tfh cells. Moreover, we demonstrated that extended immunization reduced the functional responses of $CD4^+$ and $CD8^+$T cells, restrained the population of memory T cells, and up-regulated the expression of PD-1 and LAG-3 in Te sub-type cells. An increased percentile of Treg cells was also observed, accompanied by significant elevation of IL-10 production. Together, we provided crucial evidence that repetitive administration of RBD booster vaccines may negatively impact the immune response established by a conventional vaccination course and promote adaptive immune tolerance.

In our recent study, a three-dose course of RBD vaccines successfully yielded both humoral and cellular immune protection for 4 months in a Balb/c mice model (Gao et al., 2021). In the current study, we found that a subsequent fourth administration of the same vaccine continued to stimulate the production of RBD-specific neutralizing antibodies, whose serum levels were sustained for at least 6 weeks. These findings were in

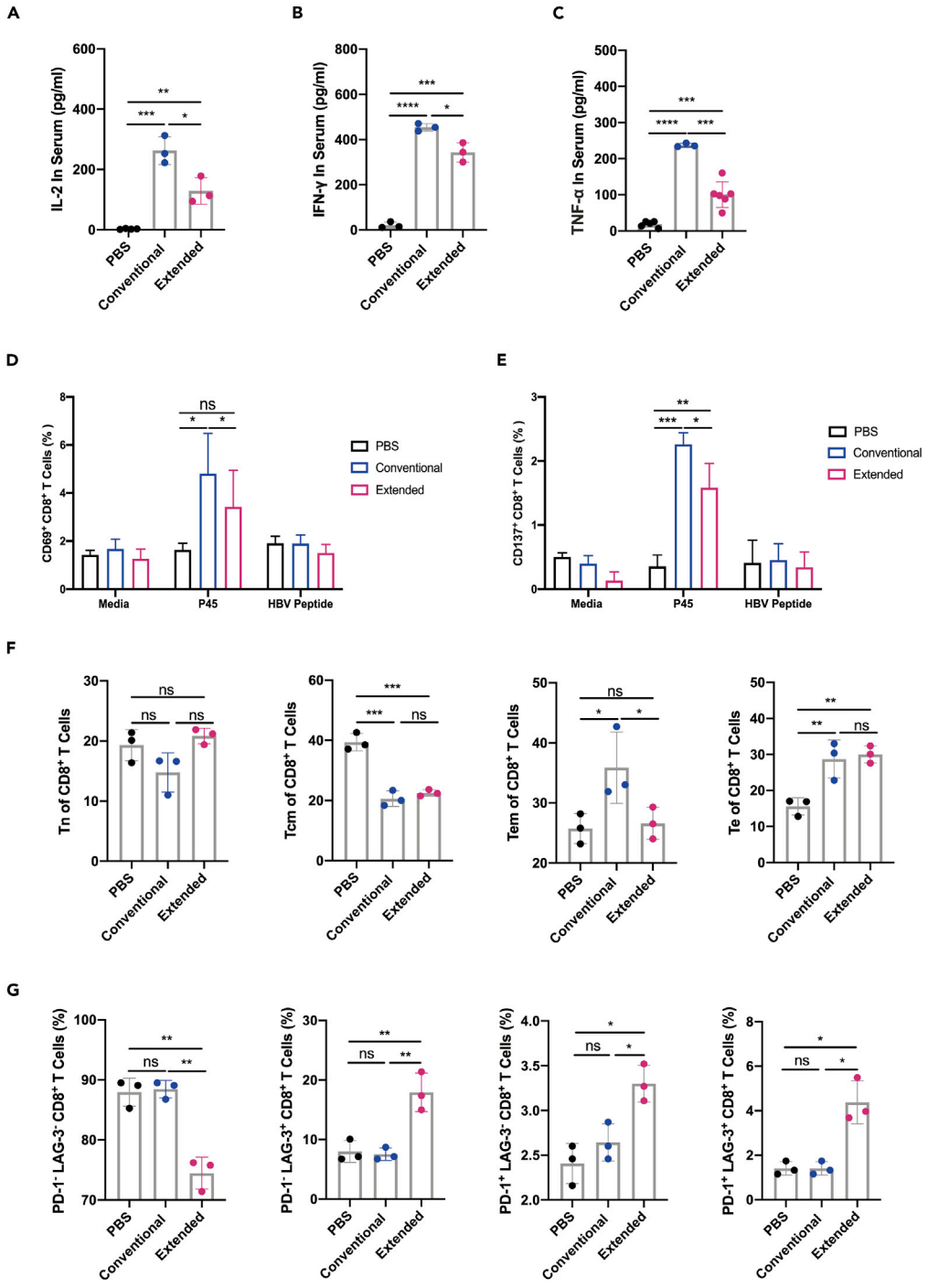

Figure 6. Extended immunization inhibited CD8$^+$ T cell-mediated immune response

IL-2 (A), IFN-γ (B) and TNF-α (C) in the immunized serum were detected on the seventh day after the last immunization. The expression of CD69 (D) and CD137 (E) in splenocytes (gated on CD8$^+$T cells) were respectively detected by flow cytometry after 10 μg/mL RBD or HBV peptide stimulation for 24 h, conventional media was used as negative control.

(F) The ratio of Tn (CD62L$^+$ CD44$^-$), Te (CD62L$^-$ CD44$^-$), Tem (CD62L$^-$ CD44$^+$) and Tcm (CD62L$^+$ CD44$^+$) of CD8$^+$T cells on day 7 after the last immunization.

(G) The expression of PD-1 and LAG-3 (gated on CD8$^+$T cells) were detected on day 7 after the last immunization. Data were presented as mean ± (SEM). *p<*0.05*, **p< 0.01, ***p< 0.001, ****p< 0.0001. ns represented non-significant.

accordance with the reported neutralizing effect of the fourth dose of the Pfizer vaccine on the SARS-CoV-2 mutants (Tanne, 2022). However, when we administrated additional doses of the same vaccine booster, with the attempt to induce a similarly enhanced or at least sustained immune response, we observed an overt reduction of the overall immune responses. Both the titer of RBD-specific antibodies and the serum neutralizing potency against SARS-CoV-2 pseudo-viruses were severely impacted, with more than two folds decrease in the IC_{50} against the most recently emerged SARS-CoV-2 variants, including the Delta and Omicron mutants. This suggests that repetitive administration of RBD booster vaccines may actively promote humoral immune tolerance, instead of functional humoral immunity. A recent independent report made similar observation that one additional booster with inactivated SARS-CoV-2 vaccine in human significantly reduced the titer of the RBD-specific antibodies, when administered at a time with already observed loss in protective efficacy (Perez-Then et al., 2022). It suggested that for booster vaccines developed targeting wild-type SARS-CoV-2 RBD, the doses or the immunization course might be a key factor that could be negatively influenced by immune tolerance. It might be of importance to monitor the serum levels of antibodies prior to any extended vaccination.

The evidenced immune tolerance from repetitive dosing with homologous boosters in our study suggests that caution should be exercised when optimizing the extended plan for SARS-CoV-2 booster vaccination. Instead of continuous dosing with homologous prime vaccines, a mid-way switch to heterologous booster choices may offer a chance of improvement to the observed energy against Omicron mutants (Reynolds et al., 2022). Such vaccination strategy may take advantage of the otherwise unsatisfying immune response consequential to the serum phenomenon termed antibody imprinting or original antigenic sin (OAS), which has been an emerging subject in SARS-CoV-2 vaccination, especially for children (Lavinder and Ippolito, 2022). Encountering heterologous boosters, the OAS-dominated immune memory response might generate a faster and stronger neutralizing protection from a preferential activation of existing B cell clones with antibodies recognizing epitopes of the wild-type strain. This might provide a window of opportunity for sufficient time and accumulation of heterologous antigens that could induce proper recruitment of new naive B cells to generate another primary or secondary response to new epitopes presented. It is reasonable to speculate that such variant-specific immune adaptation may enhance the durability and/or efficacy for the evolving protective need. Within such framework, tailored mRNA vaccines may be a good choice to circumvent the loss of effective humoral and cellular immunity from conventional vaccines developed with the wild-type virus. Given the differences between human and mice in mechanism of OAS, further studies are definitely needed to strategically optimize the application of vaccine boosters for durable protection against SARS-CoV-2.

In the attempt to explain the mechanism of humoral immune tolerance associated with our extended immunization course, we analyzed the mechanisms involved in RBD-specific antibody production. With prolonged booster vaccination to mice, we observed significantly reduced number of elementary factors and assistant T cells that would be required for B cell maturation and activation, relative to the conventional course of immunization. Insufficient availability of Tfh cells might hinder the conventional process of B cell functional differentiation, and the decreased amount of serum IL-4 might impede B cell activation. These assumptions were supported by the fact that a significantly lower number of active B cells was detected within the germinal center from mice of the extended immunization group as comparing to the animals received conventional course of vaccination. Notably, we found that the proportion of memory B cell was markedly reduced in the extended immunization group, together with signs of B cell immune tolerance, indicating the repetitive vaccination of booster shots shared similar mechanisms as seen from humoral immune tolerance of repeated antigen exposure, as during chronic viral infections (Han et al., 2013).

In addition to the humoral immune responses, cellular immune tolerance was observed during the extended course of RBD booster vaccination. Limited levels of antigen-specific memory T cell activation and profoundly decreased IL-2 and IFN-γ secretion were found in the sera of the extended group, contrast to sustained cellular immune responses after 4 dosings of RBD vaccines. It was reported that the chronic infection with HBV virus could result in antigen-specific cellular immune tolerance, which was manifested as a partial or complete inability to induce active immune response from antigen-specific $CD8^+$T cells and significant increase in the surface expressions of inhibitory receptors, including PD-1, Tim-3 and CTLA-4. Similarly, we found that prolonged administration of RBD booster vaccines overtly increased the levels of PD-1 and LAG-3, accompanied by significant reduction of the memory $CD8^+$T cells (Han et al., 2013). This is of particular importance, because memory $CD8^+$T cell response is shown to play a predominant role for effective response against newly emerged SARS-CoV-2 variants, which greatly

challenged humoral immunity with collective neutralization escape mutations (Tarke et al., 2022; Naranbhai et al., 2022; Swadling et al., 2022). Therefore, over-stimulation with the same booster vaccine or reinfection after vaccination may severely hamper the cellular immune response established by conventional vaccine course, which, together with challenged humoral immune responses, may lead to prolonged disease duration and/or aggravation of symptoms in recipients.

Moreover, over-vaccination may generate an immunosuppression micro-environment that is also an important facilitator of immune tolerance. We demonstrated that both the percentage of $CD25^{+}Foxp3^{+}CD4^{+}$ Treg cells and the levels of immunosuppression cytokines IL-10 were up-regulated after extended RBD vaccine booster vaccination. This may result in reduced activation and differentiation of B cells on antigen stimulation, as well as functional inhibition of antigen-presenting cells (APCs) and consequential decrease in $CD8^{+}$T cell activation (Damo and Joshi, 2019; Field et al., 2020; Turner et al., 2020). Indeed, we observed both humoral and cellular immune tolerance with the doses of extended booster administrations, which made it safe to speculate that over-vaccination might severely impact the immune protective efficacy established by conventional SARS-CoV-2 immunization, and probably enhance disease severity for new COVID-19 patients or re-infectants.

Although RBD subunit vaccines cannot entirely represent inactivated or mRNA vaccines, especially in antigen delivery way. A recent report in The New England Journal of Medicine demonstrated that a fourth mRNA vaccination of healthy young health care workers only shows marginal benefits (Regev-Yochay et al., 2022). Whether extended vaccination with other COVID-19 vaccines based on wild-type SARS-CoV-2 sequence will induce immune tolerance, further investigations are required.

In summary, we characterized the comprehensive effects of extended immunization with RBD booster vaccines in a balb/c mouse model. Our findings revealed that repeated dosing after the establishment of vaccine response might not further improve the antigen-specific reactivity; instead, it could cause systematic tolerance and inability to generate effective humoral and cellular immune responses to current SARS-CoV-2 variants. Our study provides timely information for the prevention of COVID-19. It puts an extended immunization course with two or more RBD-based vaccine boosters at debate, and warns for the future applications of vaccine enhancers without proper evaluation of serum antibody titers and T cell functions.

Limitations of the study

We used a rodent animal model instead of primates in this study. Although the actual kinetics of immune reactivity between mice and humans is not fully understood, the Balb/c mice model has been shown to share profound similarities with humans in response to SARS-CoV-2 infections (Halfmann et al., 2022). Thus, the observed adaptive immune tolerance associated with extended booster vaccination might present important reference value, particular for the recipients of homologous vaccines. Our published research reported that antibody titter in immunized mice serum began to decline three to four weeks after the last vaccine injection (Gao et al., 2021). Therefore, the three-week interval between boosters in this study was slightly shorter. Another limitation of this study is that we tested an extended course of vaccination in which the vaccines were administrated at a routine time interval, instead of given at a late time when the immune responses were waning as seen in vaccinees. Our results revealed the potential adverse effects associated with regular SARS-CoV-2 enhancer vaccines and highlighted the complexity of systematic immune status at the time of vaccination which could be significantly affected by adaptive tolerance. In support of our finding, a recent independent study in a 38 vaccinees cohort showed similar decrease in humoral immunity, when given a second booster of inactivated SARS-CoV-2 virus at the time of compromised immune response (Wang et al., 2022). Despite the lack of direct evidence for alterations in splenic $CD8^{+}$T cell activation, the observed decrease of CD137 and CD69 expressions in spleen-derived $CD8^{+}$T cells stimulated by P45 peptide, together with the reduction in the serum levels of effector molecules IL-2, IFN-γ and TNF-α, supported that extended immunization of RBD subunit vaccines impaired the activation of P45-specific $CD8^{+}$ cellular immunity. Collectively, these results suggest that cautions are needed with repetitive SARS-CoV-2 booster vaccination in massive scale population.

STAR★METHODS

Detailed methods are provided in the online version of this paper and include the following:

SUPPLEMENTAL INFORMATION

Supplemental information can be found online at https://doi.org/10.1016/j.isci.2022.105479.

ACKNOWLEDGMENTS

The study was supported by SARS-CoV-2 Virus Emergency Research Project of Chongqing Medical University.

AUTHOR CONTRIBUTIONS

Conceptualization and supervision, A.-S.J.; methodology, F.-X.G., R.-X.W., J.-J.H., S.-Y.S.; investigation, T.-T.L., C.H., M.-Y.S., S.-M., F.-Y.L., S.-Y.S., Y.-N.H., X.-J.H., Q.C., Y-M.W., L.L., S.-L.L.; writing-original draft, F.-X.G. and R.-X.W.; funding acquisition and resources, A.-S.J.; all authors discussed and commented on the manuscript.

DECLARATION OF INTERESTS

The authors declare no competing interests.

INCLUSION AND DIVERSITY

We support inclusive, diverse, and equitable conduct of the research.

Received: April 27, 2022
Revised: August 14, 2022
Accepted: October 28, 2022
Published: December 22, 2022

REFERENCES

Atmar, R.L., Lyke, K.E., Deming, M.E., Jackson, L.A., Branche, A.R., El Sahly, H.M., Rostad, C.A., Martin, J.M., Johnston, C., Rupp, R.E., et al. (2022). Homologous and heterologous Covid-19 booster vaccinations. N. Engl. J. Med. *386*, 1046–1057.

Cerqueira-Silva, T., de Araujo Oliveira, V., Paixão, E., S., Júnior, J., B., Penna, G., O., Werneck, G., v., Pearce, N., Barreto, M., L., Boaventura, V., S., Barral-Netto, M., et al. (2022). Duration of protection of CoronaVac plus heterologous BNT162b2 booster in the Omicron period in Brazil. Nat. Commun. *18*, 13.

Chakrabarti, S., Chakrabarti, S.S., Chandan, G., Kaur, U., and Agrawal, B.K. (2022). Effectiveness of ChAdOx1 nCoV-19 vaccine during the delta (B.1.617.2) variant surge in India. Lancet Infect. Dis. *22*, 446–447.

Cheng, S.M.S., Mok, C.K.P., Leung, Y.W.Y., Ng, S.S., Chan, K.C.K., Ko, F.W., Chen, C., Yiu, K., Lam, B.H.S., Lau, E.H.Y., et al. (2022). Neutralizing antibodies against the SARS-CoV-2 Omicron variant BA.1 following homologous and heterologous CoronaVac

or BNT162b2 vaccination. Nat. Med. *28*, 486–489.

Damo, M., and Joshi, N.S. (2019). Treg cell IL-10 and IL-35 exhaust CD8(+) T cells in tumors. Nat. Immunol. *20*, 674–675.

Elliott, T., Cheeseman, H., M., Evans, A., B., Day, S., McFarlane, L., R., O'Hara, J., Kalyan, M., Amini, F., and Cole, T. (2022). Enhanced immune responses following heterologous vaccination with self-amplifying RNA and mRNA COVID-19 vaccines. PLoS. Pathog. *10*, 18–28.

Fahrner, J.E., Lahmar, I., Goubet, A.G., Haddad, Y., Carrier, A., Mazzenga, M., Drubay, D., Alves Costa Silva, C.; Lyon COVID Study Group, and de Sousa, E., et al. (2022). The polarity and specificity of antiviral T lymphocyte responses determine susceptibility to SARS-CoV-2 infection in patients with cancer and healthy individuals. Cancer Discov. *12*, 958–983.

Field, C.S., Baixauli, F., Kyle, R.L., Puleston, D.J., Cameron, A.M., Sanin, D.E., Hippen, K.L., Loschi, M., Thangavelu, G., Corrado, M., et al. (2020). Mitochondrial integrity regulated by lipid metabolism is a cell-intrinsic checkpoint for Treg suppressive function. Cell Metab. *31*, 422–437.e5.

Gao, F., Huang, J., Li, T., Hu, C., Shen, M., Mu, S., Luo, F., Song, S., Hao, Y., Wang, W., et al. (2021). A highly conserved peptide vaccine candidate activates both humoral and cellular immunity against SARS-CoV-2 variant strains. Front. Immunol. *12*, 789905.

Gruell, H., Vanshylla, K., Tober-Lau, P., Hillus, D., Schommers, P., Lehmann, C., Kurth, F., Sander, L.E., and Klein, F. (2022). mRNA booster immunization elicits potent neutralizing serum activity against the SARS-CoV-2 Omicron variant. Nat. Med. *28*, 477–480.

Halfmann, P., J., Iida, S., Iwatsuki-Horimoto, K., Maemura, T., Kiso, M., Scheaffer, S., M., Darling, T., L., Joshi, A., Loeber, S., Singh, G., et al. (2022). SARS-CoV-2 Omicron virus causes attenuated disease in mice and hamsters. Nature *603*, 7902.

Han, Q., Lan, P., Zhang, J., Zhang, C., and Tian, Z. (2013). Reversal of hepatitis B virus-induced systemic immune tolerance by intrinsic innate immune stimulation. J. Gastroenterol. Hepatol. *28*, 132–137.

Lavinder, J.J., and Ippolito, G.C. (2022). Boosted immunity to the common cold might protect children from COVID-19. Nat. Immunol. *23*, 8–10.

Lederer, K., Bettini, E., Parvathaneni, K., Painter, M.M., Agarwal, D., Lundgreen, K.A., Weirick, M., Muralidharan, K., Castaño, D., Goel, R.R., et al. (2022). Germinal center responses to SARS-CoV-2 mRNA vaccines in healthy and immunocompromised individuals. Cell *185*, 1008–1024.e15.

Lin, Y., Goebels, J., Xia, G., Ji, P., Vandeputte, M., and Waer, M. (1998). Induction of specific transplantation tolerance across xenogeneic barriers in the T-independent immune compartment. Nat. Med. *4*, 173–180.

Naranbhai, V., Nathan, A., Kaseke, C., Berrios, C., Khatri, A., Choi, S., Getz, M.A., Tano-Menka, R., Ofoman, O., Gayton, A., et al. (2022). T cell reactivity to the SARS-CoV-2 Omicron variant is preserved in most but not all individuals. Cell *185*, 1259.

Perez-Then, E., Lucas, C., Monteiro, V.S., Miric, M., Brache, V., Cochon, L., Vogels, C.B.F., Malik, A.A., De la Cruz, E., Jorge, A., et al. (2022). Neutralizing antibodies against the SARS-CoV-2 Delta and Omicron variants following heterologous CoronaVac plus BNT162b2 booster vaccination. Nat. Med. *28*, 481–485.

Regev-Yochay, G., Gonen, T., Gilboa, M., Mandelboim, M., Indenbaum, V., Amit, S., Meltzer, L., Asraf, K., Cohen, C., Fluss, R., et al. (2022). Efficacy of a fourth dose of Covid-19 mRNA vaccine against Omicron. N. Engl. J. Med. *386*, 1377–1380.

Reynolds, C.J., Pade, C., Gibbons, J.M., Otter, A.D., Lin, K.M., Muñoz Sandoval, D., Pieper, F.P., Butler, D.K., Liu, S., Joy, G., et al. (2022). Immune boosting by B.1.1.529 Omicron) depends on previous SARS-CoV-2 exposure. Science *377*, eabq1841.

Rizzuto, G., Brooks, J.F., Tuomivaara, S.T., McIntyre, T.I., Ma, S., Rideaux, D., Zikherman, J., Fisher, S.J., and Erlebacher, A. (2022). Establishment of fetomaternal tolerance through glycan-mediated B cell suppression. Nature *603*, 497–502.

Swadling, L., Diniz, M., O., Schmidt, N., M., Amin, O., E., Chandran, A., Shaw, E., Pade, C., Gibbons, J., M., Le Bert, N., Tan, A., T., et al. (2022). Pre-existing polymerase-specific T cells expand in abortive seronegative SARS-CoV-2. Nature *601*, 7891.

Tanne, J.H. (2022). Covid-19: Pfizer asks US regulator to authorise fourth vaccine dose for over 65s. BMJ *376*, o711.

Tarke, A., Coelho, C., H., Zhang, Z., Dan, J., M., Yu, E., D., Methot, N., Bloom, N., I., Goodwin, B., Phillips, E., Mallal, S., et al. (2022). SARS-CoV-2 vaccination induces immunological T cell memory able to cross-recognize variants from Alpha to Omicron. Cell *3*, 185.

Thiruvengadam, R., Awasthi, A., Medigeshi, G., Bhattacharya, S., Mani, S., Sivasubbu, S., Shrivastava, T., Samal, S., Rathna Murugesan, D., Koundinya Desiraju, B., et al. (2022). Effectiveness of ChAdOx1 nCoV-19 vaccine against SARS-CoV-2 infection during the delta (B.1.617.2) variant surge in India: a test-negative, case-control study and a mechanistic study of post-vaccination immune responses. Lancet Infect. Dis. *22*, 473–482.

Turner, J.A., Stephen-Victor, E., Wang, S., Rivas, M.N., Abdel-Gadir, A., Harb, H., Cui, Y., Fanny, M., Charbonnier, L.M., Fong, J.J.H., et al. (2020). Regulatory T cell-derived TGF-beta1 controls multiple checkpoints governing allergy and autoimmunity. Immunity *53*, 1202–1214.e6.

Walls, A.C., Sprouse, K.R., Bowen, J.E., Joshi, A., Franko, N., Navarro, M.J., Stewart, C., Cameroni, E., McCallum, M., Goecker, E.A., et al. (2022). SARS-CoV-2 breakthrough infections elicit potent, broad, and durable neutralizing antibody responses. Cell *185*, 872–880.e3.

Wang, J., Deng, C., Liu, M., Liu, Y., Li, L., Huang, Z., Shang, L., Jiang, J., Li, Y., R, M., et al. (2022). Four doses of the inactivated SARS-CoV-2 vaccine redistribute humoral immune responses away from the Receptor Binding Domain. Preprint at medRxiv. https://doi.org/10.1101/2022.02.19.22271215.

Young, C., and Brink, R. (2021). The unique biology of germinal center B cells. Immunity *54*, 1652–1664.

Zhou, D., Dejnirattisai, W., Supasa, P., Liu, C., Mentzer, A.J., Ginn, H.M., Zhao, Y., Duyvesteyn, H.M.E., Tuekprakhon, A., Nutalai, R., et al. (2021). Evidence of escape of SARS-CoV-2 variant B.1.351 from natural and vaccine-induced sera. Cell *184*, 2348–2361.e6.

STAR★METHODS

KEY RESOURCES TABLE

REAGENT or RESOURCE	SOURCE	IDENTIFIER
Antibodies		
APC anti-mouse CD19	BioLegend	Cat#152409; AB_2629838
PE anti-mouse CD138	BioLegend	Cat#142503; AB_10915989
FITC anti-mouse/rat/human CD27	BioLegend	Cat#124207; AB_1236463
PE/Cyanine7 anti-mouse CD4	BioLegend	Cat#100421; AB_312706
APC/Cyanine7 anti-mouse CD185 (CXCR5)	BioLegend	Cat#145525; AB_2566798
PE anti-mouse CD279 (PD-1)	BioLegend	Cat#135205; AB_1877232
FITC anti-mouse/human GL7 Antigen	BioLegend	Cat#144603; AB_2561696
PerCP/Cyanine5.5 anti-mouse CD95 (Fas)	BioLegend	Cat#152609; AB_2632904
Alexa Fluor® 647 anti-mouse/human CD45R/B220 Antibody	BioLegend	Cat#103229; AB_492875
Alexa Fluor 700 anti-mouse CD3	BioLegend	Cat#100216; AB_493697
PE anti-mouse CD8a	BioLegend	Cat#162303; AB_2894434
Brilliant Violet 605™ anti-mouse CD69	BioLegend	Cat#104529;AB_11203710
APC anti-mouse CD137	BioLegend	Cat#106109; AB_2564296
APC anti-mouse CD279	BioLegend	Cat#109111; AB_10613470
PE anti-mouse CD223	BioLegend	Cat#125208; AB_2133343
Brilliant Violet 605™ anti-mouse/human CD44	BioLegend	Cat#103047; AB_2562451
Brilliant Violet 421™ anti-mouse CD62L	BioLegend	Cat#104435; AB_10900082
Alexa Fluor® 488 anti-mouse FOXP3	BioLegend	Cat#136803; AB_10946412
HRP-conjugated Goat Anti-Mouse IgG H&L secondary antibody	Abcam	Cat#ab6789; AB_955439
HRP-conjugated Goat Anti-Mouse IgG1 H&L	Bethyl	Cat#A90-105P; AB_67150
HRP-conjugated Goat Anti-Mouse IgG2a H&L	Bethyl	Cat#A90-107P; AB_67155
Goat anti-mouse IgG-ALP	MabTech	Cat#3310-4; AB_2890180
Bacterial and virus strains		
SARS-COV-2-S	GenBank	QVE75681.1
SARS-CoV-2-S$^{B.1.617.2}$	GenBank	EPI_ISL_4299998
SARS-COV-2-S^{Omicron}	GenBank	EPI_ISL_7263803
Biological samples		
RBD recombination protein	Stored in the lab	N/A
Chemicals, peptides, and recombinant proteins		
RBD-his protein	Sinobiological	Cat#40592-V05H
RBD-mfc protein	Sinobiological	Cat#40592-V05H
ACE2-his protein	Sinobiological	Cat#10108-H08H
Critical commercial assays		
LIVE/DEADTM Fixable Dead Cell Stain Kit	Invitrogen	Cat#L34976
Mouse and Rat cytokine Assays kit	Bio-RAD	Cat#10014905
Experimental models: Cell lines		
HEK 293T	ATCC	N/A
293F cells	ATCC	N/A

(*Continued on next page*)

Continued

REAGENT or RESOURCE	SOURCE	IDENTIFIER
Experimental models: Organisms/strains		
Balb/c mice; females	Experimental Animal Center of Chongqing Medical University	N/A
Software and algorithms		
Graphpad Prism 8	Graphpad Prism 8	N/A
Flow jo version 10.5.2.	Flow jo version 10.5.2.	N/A
Other		
6-well cell culture plates	Thermo Fisher	Cat#140675
Corning CellBIND Surface 100 mm Culture Dish	Corning	Cat#3296
Bio-plex mouse cytokines detection kit	Bio-rad	Cat#M60000007A
ELISPOT plates	Thermo Fisher	Cat#AB2384B

RESOURCE AVAILABILITY

Lead contact

Requests for resources and reagents should be directed to the lead contact A.-S.J. (aishunjin@cqmu.edu.cn).

Materials availability

All reagents and materials will be made available on request after completion of a Materials Transfer Agreemen.

Data and code availability

This study did not generate original code. Any additional information required to reanalyze the data reported in this paper is available from the lead contact upon request. All data produced in this study are included in the published article and its supplementary information, or are available from the lead contact upon request.

EXPERIMENTAL MODEL AND SUBJECT DETAILS

Cell lines

We obtained HEK 293T and 293F cells from the AmericanType Culture Collection (ATCC). Daudi cells and ACE2-HEK 293T cells were kept in our lab. HEK 293T and HACE2-293T cells were cultured in Dulbecco modified Eagle medium (Gibco^{TM}, USA) supplemented with 10% fetal bovine serum (Gibco, USA), 100 mg/mL streptomycin, and 100 U/mL penicillin at 37°C and 5% CO2. Daudi cells were cultured in DMEM media supplemented with 10% fetal bovine serum (Gibco^{TM}, USA), 100 mg/mL streptomycin, and 100 U/mL penicillin at 37°C and 5% CO_2.

Plasmids

- *pWPXL*, *pMD2.G* and *pSPAX2* in this study have been deposited to Center for immunology research of Chongqing Medical University.
- The EcoR I restriction site of the pMD2.G vector was synthesized and cloned into SARS-COV-S with 19 amino acids missing at the carbon end.
- The pWPXL luciferase reporter vector (pWPXL-luciferase) constructed by N. Landau was provided by Prof. Chiguo Cai of Wuhan University (Wuhan, China).
- The plasmid pMD2.G expressing VSV-G was provided by Prof. Ding Xue of Tsinghua University (Beijing, China).
- The expression plasmid of human ACE2 was obtained from GeneCopoeia (Guangzhou, China).

RBD protein production and purification

Ersi1919-514 aa was cloned into the mammalian expression vector pcDNA 3.4, which expresses the wild-type SARS-CoV-2 RBD protein (residue 334–526), which is located upstream of the mouse IgG signaling peptide, AviTag and a 6×His tag. The SARS-CoV-2 RBD recombinant protein was expressed in 293F cells (ATCC) for 7 days before being purified using affinity chromatography with a HisTrap column (GE Healthcare).

Mouse strains

Balb/c mice used in this study have been deposited to Animal research center of Chongqing Medical University. Mice were group-housed by randomly in individually ventilated cages Mice were maintained on a 12:12 light cycle at 30–70% humidity and provided sulfatrim-containing water and standard chow diets.

METHOD DETAILS

Institutional approvals

All animal experiments described in this study were reviewed and approved by the Institutional Animal Care and Use and Committee of Chongqing Medical University (CQMU202104).

Mice immunization strategy

50 μg RBD recombinant protein (Sinobiological: #40592-V05H) was dissolved in 100 μL PBS and then formulated in Freund's complete adjuvant (Sigma: #9007-81-2) or Freund's incomplete adjuvant (Sigma: #F5506-10ML) at a ratio of 1.2:1. Four subcutaneous immunizations were administered in conventional group (at Weeks 0, 2, 4, and 6). Or six subcutaneous immunizations were administered in extended group (at Weeks 0, 2, 4, 6, 9, and 12). On day 10 after each immunization, tail vein blood was collected and immediately used for antibody analysis.

Serum ELISA

RBD-specific IgG, IgG1 and IgG2a antibody titers in immunized mice serum were detected by ELISA. 20 μL RBD protein (Sinobiological: #40592-V05H, 3 μg/mL) were added to the 384-well plate and then incubated overnight at 4°C. After washing, the plates were blocked with blocking buffer (5% BSA plus 0.05% Tween 20) at 37°C for 1 hour and incubated with 20μL testing mice serum with ten-fold serial dilutions at 37°C for half an hour. Reacted mice serum were detected using HRP-conjugated Goat Anti-Mouse IgG H&L secondary antibody (Abcam: #ab6789, 1: 10000), HRP-conjugated Goat Anti-Mouse IgG1 H&L (Bethyl: #A90-105P, 1: 10000) and HRP-conjugated Goat Anti-Mouse IgG2a H&L (Bethyl: #A90-107P, 1: 10000) respectively.

IgG ELISPOT

Mouse splenocytes were stimulated with R848 (Sigma: #SML0196-10MG, 2 μg/mL) and mouse IL-2 (PeproTech: #212-12-20UG, 100U/mL) for six days to induce memory B cells differentiate into plasma cells. IgG ELISPOT assay was performed as reported and with minor modification (Gao et al., 2021). 35% alcohol with sterile water were used to activate the ELISPOT plates (Millipore: #0038401-5) less than 1 minute and discarded liquid. 50 μL RBD (Sinobiological: #40592-V05H,10 mg/mL) were added to the plates overnight at 4°C. Then, 5×10^5/well plenocytes were seeded in plates and stimulated for 36 hours with RBD protein (Sinobiological: #40592-V05H,10 mg/mL). Stimulation with an equimolar volume of media was performed as the negative control. Subsequently, the plates were developed with Goat anti-mouse IgG-ALP (MabTech: #3310-4, 1:1000). IgG spots were developed by the BCIP/NBT plus substrate (MabTech: #3650-10, 50μL) and quantified with the AID ELISPOT Reader (AID, Germany). To quantify positive RBD-specific responses, results were expressed as the numbers of RBD-specific IgG spots per 5×10^5 splenocytes of each mouse. IgG spots = (RBD-stimulated well # 1 - unstimulated well # 1) + (RBD-stimulated well # 2-unstimulated well # 2)/2.

Immunofluorescence

The spleens of immunized mice were separated on day 7 after the final immunization and embedded in Optimal Cutting Temperature (O.C.T) compound (SAKURA: #4583). The tissues were frozen at liquid nitrogen before sectioning (7 um) on a cryostat. After being fixed in cold acetone and blocked with 5% FBS in PBS at room temperature (RT) for 1 hour, the sections were incubated with Biotinylated PNA (VECTOR: #FL-1071-5, 1: 100) overnight at 4°C. DyLight 488 Streptavidin (BioLegend: #405218, 1: 100) was used as

the secondary antibody at RT for 1 hour followed with Alexa Fluor647-conjugated anti-mouse CD45R (BioLegend: #103226,1: 150) at RT for 1 hour. After staining, the sections were scanned under a Pannoramic SCAN instrument (3DHISTECH, Hungary).

Flow cytometric analysis

Lymphocytes from blood or spleen of immunized mice were harvested on day 7 after the last immunization and analyzed by flow cytometry. Dead cells were excluded by viability dye staining, and adherent cells were excluded by SSC/A and SSC/H gating analysis. Cells were analyzed by a BD LSRFortessa™ Flow Cytometry (BD Biosciences, USA). Data were acquired and analyzed by Flow jo version 10.5.2. LIVE/DEADTM Fixable Dead Cell Stain Kit (Invitrogen: #L34976) was used for viability dye staining. For surface staining, splenocytes were stained with the following antibodies: APC anti-mouse CD19 (Clone: 1D3/CD19, Biolegend), PE anti-mouse CD138 (Syndecan-1) (Clone: 281-2, Biolegend), FITC anti-mouse/rat/human CD27 (Clone: LG.3A10, Biolegend), PE anti-mouse CD279 (PD-1) (Clone: 29F.1A1, Biolegend), PE/Cyanine7 anti-mouse CD4 (Clone: GK1.5, Biolegend), and APC/Cyanine7 anti-mouse CD185 (CXCR5) (Clone: L138D7, Biolegend) for Tfh cell analysis; with FITC anti-mouse/human GL7 Antigen (Clone: GL7, Biolegend), PerCP/Cyanine5.5 anti-mouse CD95 (Fas), (Clone: SA367H8, Biolegend), and Alexa Fluor® 647 anti-mouse/human CD45R/B220(Clone: RA3-6B2, BD Pharmingen™) mAb for GC B cell analysis. Alexa Fluor 700 anti-mouse CD3 (Clone: 17A2, Biolegend), PE anti-mouse CD8a (Clone: 53-6.7, Biolegend), Brilliant Violet 605™ anti-mouse CD69 (Clone: H1.2F3, Biolegend), APC anti-mouse CD137(Clone: H1.2F3, Biolegend), APC anti-mouse CD279 (Clone: RMP1-30, Biolegend), PE anti-mouse CD223 (Clone: C9B7W, Biolegend), Brilliant Violet 605™ anti-mouse/human CD44 (Clone: IM7, Biolegend), Brilliant Violet 421™ anti-mouse CD62L(Clone: MEL-14, Biolegend). For intracellular staining, Alexa Fluor® 488 anti-mouse FOXP3 (Clone: MF-14, Biolegend).

Collect spleen cells and wash 1× in Staining Buffer. Spin 5 minutes at 500 × *g*. After aspirating supernatant, resuspend cell pellet in 100 μL of Staining Buffer containing an optimal concentration of fluorochrome-conjugated antibodies specific for cell surface antigens. Incubate for 20 minutes at RT in dark and next wash 1× in Staining Buffer. Fix and permeabilize cells by adding 500 μL of Fixation/Permeabilization solution (BD: #554714) and next incubate at RT in the dark for 20 minutes. Spin 5 minutes, 500 × *g*. After aspirating supernatant, resuspend cell pellet in 100 μL BD Perm/Wash™ buffer containing an optimal concentration of fluorochrome-conjugated anti-cytokines antibody for intracellular staining. Stain for 30 minutes at RT in the dark. Wash cells by adding 2 mL BD Perm/Wash™ buffer. Spin 5 minutes, 500 × *g*. Aspirate supernatant. Resuspend cell pellet in 500 μL PBS and analyze by flow cytometry.

Production and titration detection of SARS-CoV-2 Pseudo-viruses

pVSVG expressing SARS-CoV-2 spike (S) protein was constructed as using the VSV-G pseudotyped ΔG-luciferase plasmid. It encoded either the S protein of SARS-CoV-2, B.1.617.2 and Omicron (BA.1) was generated. Lenti-X293T cells were grown to 70% confluency before transfection with mix plasmids of VSV-G pseudotyped ΔG-luciferase, pWPXL and pSPAX2. These cells were cultured overnight at 37°C with 5% CO_2. DMEM (Gbico, USA) supplemented with 5% fetal bovine serum (Gbico, USA) and 100 IU/mL of penicillin (beyotimem, China) and 100 μg/mL of streptomycin (beyotimem, China) was added to the inoculated cells, which were cultured overnight for 48 hours. The supernatant was harvested, filtered by 0.45 μm filter and centrifuged at 300 *g* for 7 minutes to collect the supernatant, then aliquoted and storied at −80°C. The titers of the pseudo-viruses were detected by Lenti-X qRT-PCR Titration Kit (Takara, Japan), according to the manufacturer's instructions.

Pseudo-viruses neutralization assay

Pseudo-viruses and mouse serum were generated as described above. The 50 μL serial diluted mice serum were incubated with pseudo-viruses (1×10^9 copies/mL) at 37°C for 1 hour. These pseudo virus-serum mixtures were added to co-culture with hACE2-293T cells. After 72 hours, the luciferase activities of hACE2-293T cells were analyzed by the Bright-Luciferase Reporter Assay System (Promega, China). Relative luminescence unit of Luc activity was detected using the ThermoFisher LUX reader (ThermoFisher, USA). All experiments were performed at least three times and expressed as means ± SEM. Half-maximal inhibitory concentrations (IC_{50}) of dilution folds were calculated using the Dose-response-inhibition-variable slope four-parameter logistic regression in GraphPad Prism 8.0.

Competitive ELISA

20 μL of RBD mfc protein (Sinobiological: #40592-V05H) was added to a 384-well plate (Corning: # 3570) to a final concentration of 0.2 μg/mL at 4°C overnight. The next day, the plate was blocked with blocking buffer (5% BSA plus 0.05% Tween 20) for 1 hour. Then, 20 mL of mouse serum per well and 5-fold serial dilutions were added to the dishes, incubated at 37°C for 40 minutes, and an additional the same volume of 0.2 μg/mL ACE2-his protein (Sinobiological: #10108-H08H) was added incubated at 37°C for 40 minutes. After washing with PBS, goat anti-mouse IgG H&L secondary antibody (Abcam: #ab6789, 1:10000) was incubated with the plates for 30 minutes at RT. TMB (MabTech: #3652-F10) was added to the plate, stopped with 1 mol/L HCl, and then quantitatively detected. The half-maximal inhibitory concentration (IC_{50}) was determined by using four-parameter logistic regression. The percentage of inhibition was calculated as follows: % inhibition = [(A-Blank)-(P-Blank)]/(A-Blank) × 100, where A is the maximum OD signal of RBD binding to ACE2-his when no serum was present, and P is the OD signal of RBD binding to ACE2-his in the presence of serum at a given dilution.

Cytokines assay

Mice serum were diluted 1:4 with Bio-Plex sample diluent (Bio-RAD, Mouse and Rat cytokines Assays kit: #10014905). Vortex the diluted (1×) beads for 20s and add 50 μL to each well of the assay plate. Wash the plate two times with 100 μL Bio-Plex Wash Buffer. Add 50 μL samples, standards and blank to each well incubate on shaker at 850rpmat RT for 30 minutes. Then, wash the plate three times with 100 μL wash buffer and add 25 μL the diluted (1×) detection antibodies to each well incubate on shaker at 850rpmat RT for 30 minutes. After washing, add 50 μL the diluted (1×) SA-PE to each well incubate on shaker at 850rpmat RT for 30 minutes. Wash the plate three times with 100 μL wash buffer. Resuspend beads in 125 μL assay buffer and shake the plate at 850 rpm for 30 seconds. Remove sealing tape and read the plate using the settings below.

QUANTIFICATION AND STATISTICAL ANALYSIS

The data was statistically analyzed using the GraphPad Prism version 8.0 software. The numerical results are presented as mean standard deviation. Quantitative data in histograms, line charts and individual data points were presented as mean ± SEM. Statistical analyses were performed using two-tailed unpaired Student's t-tests. $p < 0.05$ was the criterion for statistically significant group differences.